Recovery of high-qualitied Genomes from a deep-inland Salt Lake Using BASALT

Ke Yu[1#,*], Zhiguang Qiu[1#], Rong Mu[1#], Xuejiao Qiao[1#], Liyu Zhang[1#],Chun-Ang Lian[1], Chunfang Deng[1], Yang Wu[1], Zheng Xu[2],Bing Li[3], Baozhu Pan[4], Yunzeng Zhang[5], Lu Fan[6], Yong-xin Liu[7], Huiluo Cao[8], Tao Jin[9], Baowei Chen[10], Fan Wang[11], Yan Yan[12], Luhua Xie[12], Lijie Zhou[13], Shan Yi[14], Song Chi[15], Chuanlun Zhang[6], Tong Zhang[16], Weiqin Zhuang[17]

[1] School of Environment and Energy, Shenzhen Graduate School, Peking University, Shenzhen, 518055, China.
[2] School of Biotechnology and Biomolecular Sciences, University of New South Wales, Sydney, NSW 2052, Australia
[3] Guangdong Provincial Engineering Research Center for Urban Water Recycling and Environmental Safety, Tsinghua Shenzhen International Graduate School, Tsinghua University, Shenzhen, 518055, China.
[4] State Key Laboratory of Eco-hydraulics in Northwest Arid Region of China, Xi'an University of Technology, Xi'an, Shaanxi, 710048, China.
[5] Joint International Research Laboratory of Agriculture and Agri-Product Safety, the Ministry of Education of China, Yangzhou University, Yangzhou, 225009, China.
[6] Department of Ocean Science and Engineering, Southern University of Science and Technology, Shenzhen, China.
[7] State Key Laboratory of Plant Genomics, Institute of Genetics and Developmental Biology, Innovation Academy for Seed Design, Chinese Academy of Sciences, Beijing, China.
[8] Department of Microbiology, University of Hong Kong, Hong Kong, 999077, China.
[9] Guangdong Magigene Biotechnology Co., Ltd, Guangzhou, China.
[10] Southern Marine Science and Engineering Guangdong Laboratory (Zhuhai), School of Marine Sciences, Sun Yat-sen University, Zhuhai, 510275, China.
[11] School of Atmospheric Sciences, Sun Yat-sen University, Zhuhai, 519082, China.
[12] Key Laboratory of Ocean and Marginal Sea Geology, Guangzhou Institute of Geochemistry, Chinese Academy of Sciences, Guangzhou, 510640, China.
[13] College of Chemistry and Environmental Engineering, Shenzhen University, Shenzhen 518060, China.
[14] Department of Chemical and Materials Engineering, Faculty of Engineering, University of Auckland, New Zealand.
[15] Wuhan Benagen Tech Solutions Company Limited, Wuhan 430070, China.
[16] Environmental Biotechnology Laboratory, Department of Civil Engineering, The University of Hong Kong, Pokfulam Road, Hong Kong, 999077, China.
[17] Department of Civil and Environmental Engineering, Faculty of Engineering, University of Auckland, New Zealand.

Abstract

Metagenomic binning enables the in-depth characterization of microorganisms. To improve the resolution and efficiency of metagenomic binning, BASALT (Binning Across a Series of AssembLies Toolkit), a novel binning toolkit was present in this study, which recovers, compares and optimizes metagenomic assembled genomes (MAGs) across a series of assemblies from short-read, long-read or hybrid strategies. BASALT incorporates self-designed algorithms which automates the separation of redundant bins, elongate and refine best bins and improve contiguity. Evaluation using Critical Assessment of Metagenome Interpretation (CAMI) datasets at low (132 genomes) and medium (596 genomes) complexities revealed that BASALT auto-binning gained up to 10 times of shared MAGs with better quality when pairwise comparing to DASTool, VAMB and metaWRAP, resulting in up to 51% more MAGs obtained than other binners. Using BASALT, a case-study analysis of a Salt Lake sediment microbial community from northwest arid region of China was performed, resulting in 426 non-redundant MAGs, including 352 bacterial and 69 archaeal MAGs which could not be assigned to any known species from GTDB (ANI < 95%). In addition, two Lokiarchaeotal MAGs that belong to superphylum Asgardarchaeota were observed from Salt Lake sediment samples. This is the first time that candidate species from phylum Lokiarchaeota was found in the arid and deep-inland environment, filling the current knowledge gap of earth microbiome. Overall, BASALT is proven to be a robust toolkit for metagenomic binning, and more importantly, expand the Tree of Life.

Keywords: Microbiome; Metagenome; Binning refinement; Tree of Life; Salt Lake; Asgardarchaeota/Lokiarchaeota

*Contact Information:
Name: Ke Yu,
Address: Shenzhen Graduate School, Peking University, Lishui Road, Nanshan district, Shenzhen
Email: yuke.sz@pku.edu.cn

Introduction

Metagenomics analyses accommodated numerous of approaches exploring microbial diversities, biosynthetic potentials and evolutionary relationships of earth's microbiome (Tyson et al. 2004, Temperton and Giovannoni 2012). Specifically, the development of sequencing technologies, computational capacities and bioinformatic tools enabled genome-scale analyses, which freed our cognition of microorganisms from only cultivated isolates and significantly boosted our understandings on uncultivable microorganisms (Parks et al. 2017, Pasolli et al. 2019). Genome-resolved metagenomics was firstly applied in 2004 from low microbial diversity environment (Tyson et al. 2004), followed by a series of initiations such as Earth Microbiome Project (EMP) and the European Nucleotide Archive (ENA) which enabled us to unravel the microorganisms on a global scale (Thompson et al. 2017). For example, the latest report from EMP projects revealed more than 52,000 Metagenomic Assembled Genomes (MAGs) on species level (Amid et al. 2020, Nayfach et al. 2020), consisting a wide range of samples from environments with medium to high level of microbial complexities, such as human (Pasolli et al. 2019, Almeida et al. 2021), freshwater (Ali et al. 2020), marine (Tully et al. 2018, Reji et al. 2020), engineered environment (Ransom-Jones et al. 2017, Liang et al. 2020) and soil (Kroeger et al. 2018, Nascimento Lemos et al. 2020), etc. Such studies implementing genome-resolved metagenomic approaches have largely expanded branches of microorganisms on tree of life (Hug et al. 2016). However, despite these findings, a vast majority of microorganisms remain obscured due to 1) limitation of bioinformatic tools such as assembly and binning; 2) large unexplored area/regions with specific environmental conditions; and 3) advanced cultivation methods to be developed.

Aside from the developing innovations of culturing new microorganisms (Lewis et al. 2020), major discovery of novel species was based on sequencing-based analyses. However, major impediments that hampered us from obtaining comprehensive and high-qualitied MAGs from existing sequencing datasets are assembly and binning steps (Nayfach et al. 2020). Due to the nature of next-generation

sequencing, a series of errors may occur in binning sourced from assembled short-read sequences, such as mis-clustering contigs into bins, mis-separating contigs from one genome into multiple bins, and mis-separating multiple genomes into bins sharing partial genomic sequences (Rinke et al. 2013, Yu et al. 2018, Wang et al. 2019), resulting in redundant and artificial bins that interfere the actual binning result. While the development of third generation sequencing can significantly increase the length of sequencing reads to mitigate binning errors, higher costs (e.g. Pacific Biosciences sequencing, PacBio) or error reads (e.g. Oxford Nanopore Technology, ONT) are still hindrances from acquiring intact microbial genomes with higher completeness and lower contamination (Laver et al. 2015, Wang et al. 2015). To date, the development of assembly (Bankevich et al. 2012, Peng et al. 2012, Li et al. 2015), binning (Alneberg et al. 2013, Wu et al. 2016, Kang et al. 2019, Nissen et al. 2021) and refinement tools (Song and Thomas 2017, Uritskiy et al. 2018) have allowed us recovering MAGs from relatively high diversity environments (Parks et al. 2017, Sczyrba et al. 2017), but an average of 70% of sequencing reads were still unable to be exploited on genome-resolved analyses, which proportion is even higher in more complexed environment such as soil (Howe et al. 2014, Nayfach et al. 2020). Although a growing number of bioinformatic tools have implemented algorithms on third generation sequencing datasets, such as hybrid assemblers (e.g. Unicycler, OPERA-MS, Wick et al. 2017, Bertrand et al. 2019), a systematic estimation of these tools on complexed environmental samples is crucially needed. Moreover, no study has utilized third generation sequences on post-binning approaches calibrating assembled bins and complementing genome gaps, which can maximize the exploitation of long-reads data to elevate recovered genome qualities. Therefore, to further expand tree of life, more robust assembly and binning workflows, as well as post-binning refinement methods are yet to be developed.

In addition to the demands of advanced bioinformatic tools, more investigations on remote areas/regions, especially the ones from unique environmental conditions that absent from global projects (Nayfach et al. 2020, Almeida et al. 2021) can largely expand our knowledge on earth genomic

pools. As such environmental parameters (physical, chemical and biological) have direct and indirect effect on microbial communities (Berdjeb et al. 2011, Nishiyama et al. 2018, Easson and Lopez 2019, Glasl et al. 2019), exploring uncommon environment can expand the breadth of our understanding on microbial diversity and potential functions. A few studies have already launched targeting rarely explored environments on deserts (Finstad et al. 2017), oil fields (Eze et al. 2020), hydrothermal vents (Anderson et al. 2017) and non-marine soda lakes (Vavourakis et al. 2018), but such number of investigations were still scarce to support the expansion of microbial diversity, compare to a vast majority of studies on marine, soil and human-associated microbiomes (Hoshino et al. 2020, Nascimento Lemos et al. 2020, Almeida et al. 2021).

In this study, we introduce a highly robust toolkit BASALT (Binning Across a Series of AssembLies Toolkit) to robustly recover microbial genomes from sequencing datasets using a series of innovative methodologies for assembly, binning and refinements. Firstly, BASALT uses high-throughput assembly methods to automatically assemble/co-assemble multiple files in parallel to reduce the manual input; Next, BASALT incorporates self-designed algorithms which automates the separation of redundant bins to elongate and refine best bins and improve contiguity; Further, BASALT facilitates state-of-art refinement tools using third-generation sequencing data to calibrate assembled bins and complement genome gaps that unable to be recalled from bins; Lastly, BASALT is an open frame toolkit that allows multiple integration of bioinformatic tools, which can optimize a wide range of datasets from various of assembly and binning software. Using BASALT, we performed a case study on sediment samples of Aiding Lake, Xinjiang China, a deep-inland hypersaline lake with high aridity in the surrounding area (Figure S1, Guan et al. 2020), which is different from common chlorite saline aquatic system. Based on the superior number and quality of MAGs obtained via BASALT, we present taxonomic and genetic profiles on prokaryotic microbial communities of lake sediment samples, including two Lokiarchaeota species from a recently discovered archaeal superphylum Asgardarchaeota (Zaremba-Niedzwiedzka et al. 2017) that also found in our samples. Here, we

144 highlighted that BASALT can efficiently enhance the assembly and binning processes on metagenomic
145 sequences, which allows in-depth investigations on the existing dataset by increasing overall and
146 individual MAG quality. By acquiring more high-qualitied MAGs, we could potentially unfold much
147 more knowledges on known or unknown microbial taxa, potential functions and host-microbial
148 interactions, which further expand the tree of life.

149

150 Results

151 Environment, pipeline and availability

152 BASALT is command line software based on Python scripts with a series of modules, each containing
153 one or more algorithms/programs addressing data processing or analysis. Overall, BASALT is an
154 automated program running with one command line, while a few checkpoints are set in each module
155 to accommodate users to customize their preference to start at any checkpoint as needed. Further details
156 of outlines and algorithms are available at (https://github.com/EMBL-PKU/BASALT).

157

158 BASALT workflow.

159 BASALT is a versatile toolkit that provides comprehensive pipeline from mapping, automated binning
160 to post-binning refinement that enable users to retrieve non-redundant and high-qualitied MAGs from
161 metagenome samples. Overall, BASALT contains four major modules including Automated Binning,
162 Bin Dereplication, Bin Refinement and Reassembly, where five core algorithms were implemented in
163 these modules including Core Contigs Identification, Bin depth normalization, Outlier Removal,
164 Contigs Retrieval and Restrained Overlap-Layout-Consensus (rOLC, Figure 1). As BASALT enables
165 multiple assembly or co-assembly datasets from short-read sequences (next-generation sequencing,
166 NGS) or long-read sequences (third-generation sequencing, TGS) as input files, it is expected that a
167 potential increase of reads utilization is available (Stewart et al. 2018). By importing multiple

168 sequences with coverage information, BASALT conducted automated binning using prominent tools
169 such as MetaBAT2, Maxbin2 and CONCOCT (Alneberg et al. 2013, Wu et al. 2016, Kang et al. 2019)
170 that generated hybrid bin-sets. Raw hybrid bin-sets were firstly filtered with a homebrew Bin
171 Dereplication module to remove replicated bins obtained from the same assembly. The non-redundant
172 bins of each assembly were then merged and categorized into different groups at a customized average
173 nucleotide identity (ANI) cutoff. Each group of bins were further filtered by the homebrew algorithm
174 which classifies core contigs that further enables identification of redundant bins before selecting into
175 a single, hybrid bin-set obtained from all samples. The selected bin-set was further filtered using a
176 critical Outlier Removal algorithm, which integrated coverage and tetranucleotide frequency (TNF) to
177 remove outliers by using an interquartile ranges (IQR) method with multiple thresholds. Next,
178 sequences from assembly files were retrieved by connecting with existing contigs in the OR-filtered
179 bins to create an expanded sequences pool with potential connected contigs, while BASALT compared
180 and selected the refined bins with higher quality value. Further, a restrained Overlap-Layout-
181 Consensus (rOLC) step was conducted to overlap the replicated bins obtained from different
182 assemblies into OLC-merged bins, followed by the reassembly step to generate the finalized bin-set.
183 Notably, the sequence retrieval and reassembly step allowed utilization of long-read sequences
184 obtained from TGS to complement gaps and join overlapped regions on the bins to increase
185 completeness and reduce contamination.

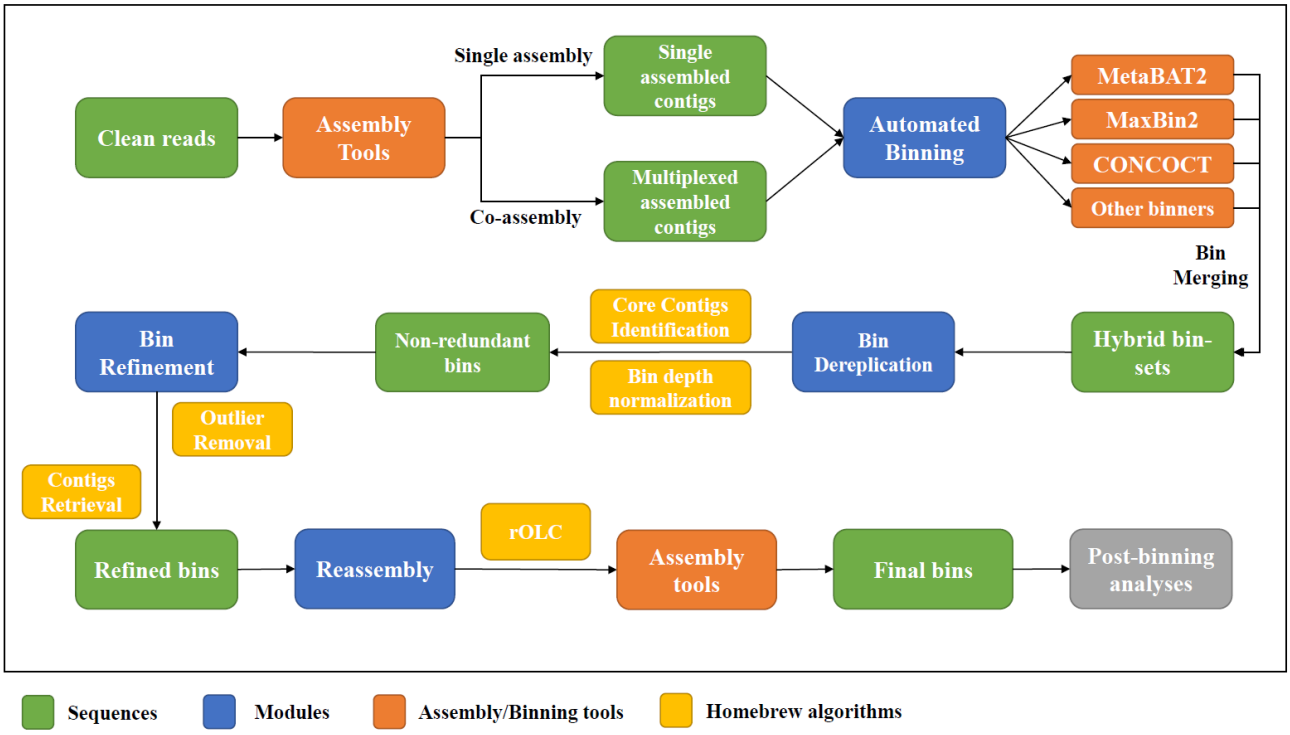

Figure 1. BASALT workflow for assembly, binning and refinement of metagenomic sequencing data (blocks in green). BASALT contains four major modules (blocks in blue) including Automated Binning, Bin Dereplication, Bin Refinement and Reassembly, where five core algorithms (blocks in yellow) were implemented in these modules including Core Contigs Identification, Bin depth normalization, Outlier Removal, Contigs Retrieval and Restrained Overlap-Layout-Consensus (rOLC). In addition to core workflow, assembly and binning tools (blocks in orange) were also flexibly embedded in BASALT.

BASALT improves recognition of non-redundant bins.

BASALT pipeline enables multiple input files for assembly, including long-reads files for hybrid assembly. The advantage of input with multiple files is not limited to the reduction of computational time but could also generate more bins than individual assembled samples. For example, binning using multiplexed samples generated 16.3%, 14.2% and 11.1% more non-redundant MAGs when using DAS Tool (MCM), VAMB and metaWRAP (MCM), respectively on CAMI-medium dataset (Table S1, Figure S2), while the increasing rate on CAMI-high dataset were 8.2%, 11.0% and 9.0%, respectively (Table S1, Figure 2A). Despite the advantage above, a major drawback using multiplexed samples was the byproducts of replicated bins, which were considered as redundant or pseudo- genomes. To address

this issue, BASALT pipeline accommodates a Bin Dereplication module with homebrew algorithms which can remove redundant bins generated from the multiplexed assemblies as well as hybrid bin-merging from automated binning, resulting in optimized, non-redundant bin-sets (Figure 1). Comparing with standard CAMI-medium and -high genomes, DAS Tool, VAMB and metaWRAP generated 85.9%, 77.1%, 95.0% (CAMI-medium) and 84.8%, 52.3%, 72.7% (CAMI-high) redundant MAGs, respectively (Figure 2A, Figure S2), while no redundancy was observed in BASALT MAGs, suggesting high redundancy rate were existed using the first three binning tools/toolkits. Remarkably, BASALT Bin Dereplication, Refinement and Reassembly modules can not only eliminate redundant MAGs generated from DAS Tool, VAMB and metaWRAP pipelines, but also increase the overall quality of non-redundant MAGs (Co-assembled data refined with BASALT, CAB, Figure 2A), suggesting good efficiently of redundancy removal and quality improvement using BASALT from co-assembled bins.

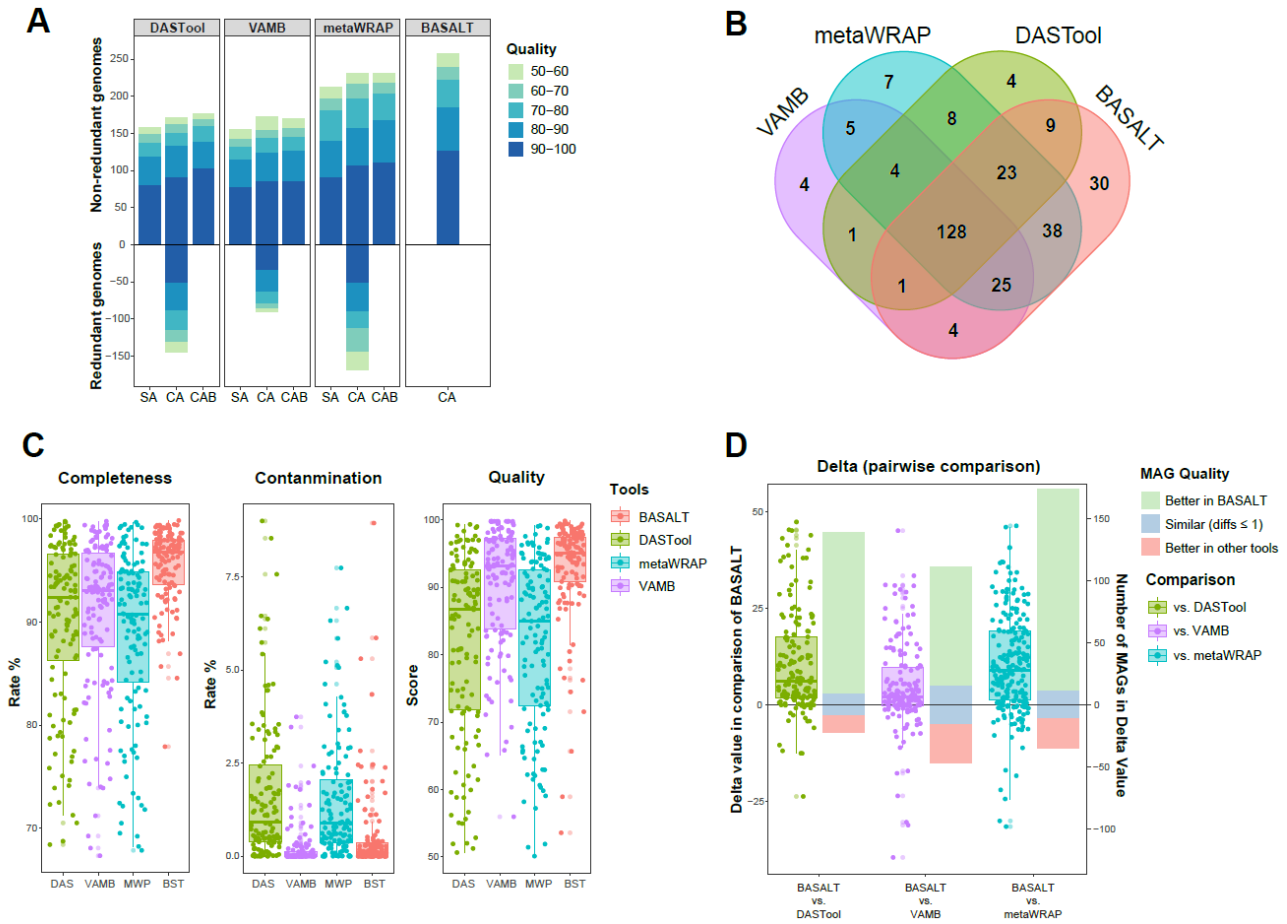

Figure 2. Comparison of BASALT with other binning tools/pipelines on CAMI-high dataset. **A)** Number of MAGs recovered from CAMI-high dataset using DASTool (MaxBin2, CONCOCT and MetaBAT2, MCM), VAMB, metaWRAP (MCM) and BASALT. In the first three tools, Co-assembly (CA) resulted in higher number of non-redundant MAGs compare to single assembly (SA) approach, while BASALT refinement module (Co-assembly refined with BASALT, CAB) removed redundant MAGs and generated higher quality of MAGs in the co-assembly approach. Color of bars indicated the quality of MAGs (50-100, from light to dark). **B)** Venn diagram showing number of MAGs recovered using different tools. There were 128 MAGs found shared across all tools, while 4, 4, 7 and 30 MAGs were uniquely recovered using DAS Tool (green), VAMB (purple), metaWRAP (cyan) and BASALT (red) pipelines, respectively. **C)** Completeness, contamination and quality of 128 shared MAGs recovered using DAS Tool (DAS, green), VAMB (purple), metaWRAP (MWP, cyan) and BASALT (BST, red). MAGs recovered using BASALT had lower contamination rate compared to DAS Tool and metaWRAP, and higher completeness and quality compared to all other tools. **D)** Pairwise comparison of MAGs shared by corresponding pairs of tools. Overall, BASALT was superior in obtaining higher qualitied MAGs compared to other tools. The number of MAGs that BASALT gained higher quality value (bars in light green) was much more than the number of MAGs that other tools gained higher quality value (bars in light red) or had similar quality value (difference of value ≤ 1, bars in light blue).

BASALT generates higher number and qualitied MAGs in synthetic microbial communities.

The BASALT refinement module not only removes redundant bins generated in other pipelines, but also improves the quality and number of MAGs. In comparison of MAGs (Quality score ≥ 50) obtained via different toolkits, BASALT resulted in 27.1%, 7.0%, 1.7% (CAMI-medium) and 50.9%, 50%, 11.7% (CAMI-high) more non-redundant MAGs than DAS Tool, VAMB and metaWRAP, respectively (Figure 2A, Figure S2, Table S1). Moreover, in top-qualitied CAMI-high MAGs (Quality score ≥ 90), BASALT obtained 38%, 47.7% and 17.6% more non-redundant MAGs than DAS Tool, VAMB and metaWRAP, respectively (Figure 2A). This result suggested BASALT is more robust retrieving high-qualitied and non-redundant MAGs from metagenome samples, especially on those samples with higher complexity.

To individually evaluate the BASALT refinement module, a further refinement step was performed on CAMI-high datasets processed with DAS Tool, VAMB and metaWRAP. Although less MAGs were

245 recovered compare to the result using comprehensive BASALT pipeline, 3.7%, 2.4% and 7.0% more
246 MAGs (Quality score ≥ 80) were retrieved, respectively, compared to the default approaches of other
247 toolkits (Table S1, Figure 2A). This result suggested that BASALT can also optimize number and
248 quality of MAGs even based on the datasets processed with other pipelines.

249 Comparing MAGs recovered from the abovementioned toolkits with reference genomes in CAMI-
250 high dataset, 128 MAGs were found universally presented across all pipelines, while 4, 4, 7 and 30
251 MAGs were uniquely recovered using DAS Tool, VAMB, metaWRAP and BASALT pipelines,
252 respectively (Figure 2B). In comparison of the 128 shared MAGs in their completeness, contamination
253 and quality score (completeness – 5*contamination) across different toolkits, BASALT has the overall
254 advantages in acquiring high-quality and low contamination MAGs in comparison with others (Figure
255 2C). Further, we performed pairwise comparison between BASALT and the other tools of shared
256 MAGs and calculated delta value (difference of MAG quality between two tools) on the same genome.
257 The delta value showed BASALT could retrieve 10, 3.1 and 6.8 times of high-quality MAGs compared
258 to DAS Tool, VAMB and metaWRAP, respectively (Figure 2D), indicating that BASALT can
259 substantially obtain better quality of MAGs comparing with other tools. In summary, BASALT can
260 retrieve a greater number of non-redundant MAGs from medium-high complexed samples with higher
261 qualities.

262

263 **BASALT efficiently retrieves genomes from high complexity samples.**

264 We performed four metagenome samples from Aiding Lake sediments using both BASALT to evaluate
265 the capacity of BASALT on improving genome qualities recovered from complexed environmental
266 samples. Using BASALT, assembled bins were quality-checked with CheckM (Parks et al. 2015),
267 resulting in 426 non-redundant MAGs (completeness – 5*contamination ≥ 50, mean completeness =
268 79%, mean contamination = 1.7%, mean quality value = 70.4), including 113 MAGs above high-

269 quality level (quality ≥ 80). As a majority of metagenomic sequences could not be utilized to recover
270 high-qualitied genomes (Nayfach et al. 2016, Nayfach et al. 2020), we estimated the efficiency of
271 sequences utilized in the lake sediment samples, resulting in 26.9% of reads mapped to the MAGs,
272 which largely improved the utilization rate of metagenomic sequences in recovered MAGs compared
273 to other samples with high complexity (Howe et al. 2014).

274 In reference to Genome Taxonomy Database (GTDB, Parks et al. 2018), all 426 MAGs from BASALT
275 pipelines were annotated spanning 39 bacterial and 8 archaeal phyla. MAGs classified into bacterial
276 phyla were mainly focused in Patescibacteria, Chloroflexota, Verrucomicrobiota, Bacterioidota,
277 Proteobacteria and Desulfobacterota, while MAGs classified into archaeal phyla were Halobacteriota,
278 Thermoplasmatota, Asgardarchaeota, Thermoproteota, Iainarchaeota and Micrarchaeota in archaeal
279 domain (Figure 3A), representing a unique characteristic of microbial communities in the Salt Lake
280 sediment. Among these 426 MAGs, 98.9% bacterial MAGs and 100% archaeal MAGs could not be
281 assigned to any known species from GTDB (ANI < 95%). At genus level, 57.6% bacterial MAGs and
282 66.7% archaeal MAGs could not be assigned to any known genus from GTDB. This result suggested
283 that there was a large repository of genetic pool to be uncovered in Salt Lake sediments.

284 To further validate the MAGs recovered from Aiding Lake sediments, we compared these assembled
285 genomes with another study by Vavourakis et al. (2018) where samples were collected from several
286 soda lakes in the Kulunda Steppe (south-western Siberia, Altai, Russia). Generally, the two datasets
287 shared a vast majority of phyla (Figure 3A), indicating that despite the different geographical location,
288 bacterial assemblages of the Salt Lakes might be similar. Specifically, diverse bacterial taxa from
289 phylum Patescibacteria were observed in our study, which paralleled with the study by Vavourakis et
290 al. (2018). On the other hand, in the unique of phyla observed in two datasets, Acidobacteriota,
291 Nitrospirota, Zixibacteria, WOR-3 and KSB31 were only present in this study (Figure 3A). In archaeal
292 communities, MAGs from phyla Halobacteriota, Thermophasmatota, Iainarchaeota and
293 Nanoarchaeota were observed in both datasets, while phyla Methanobacteriota and PWEA01 were

only present in Vavourakis et al. (2018) and phyla/superphyla Asgardarchaeota, Thermoproteota, Micrarchaeota and Aenigmatarchaeota were only present in our study (Figure 3B). In the shared phyla, a large number of MAGs from phylum Nanoarchaeota found, but only one MAG from phylum Halobacteriota observed in this study, while a large community of Halobacteriota was observed in Vavourakis et al. (2018). The difference of the two datasets might be due to the physiochemical parameters between two contrasting sites of lakes (Sorokin et al. 2014), but such differences could also be related to the different strategies of assembly, as well as binning pipelines.

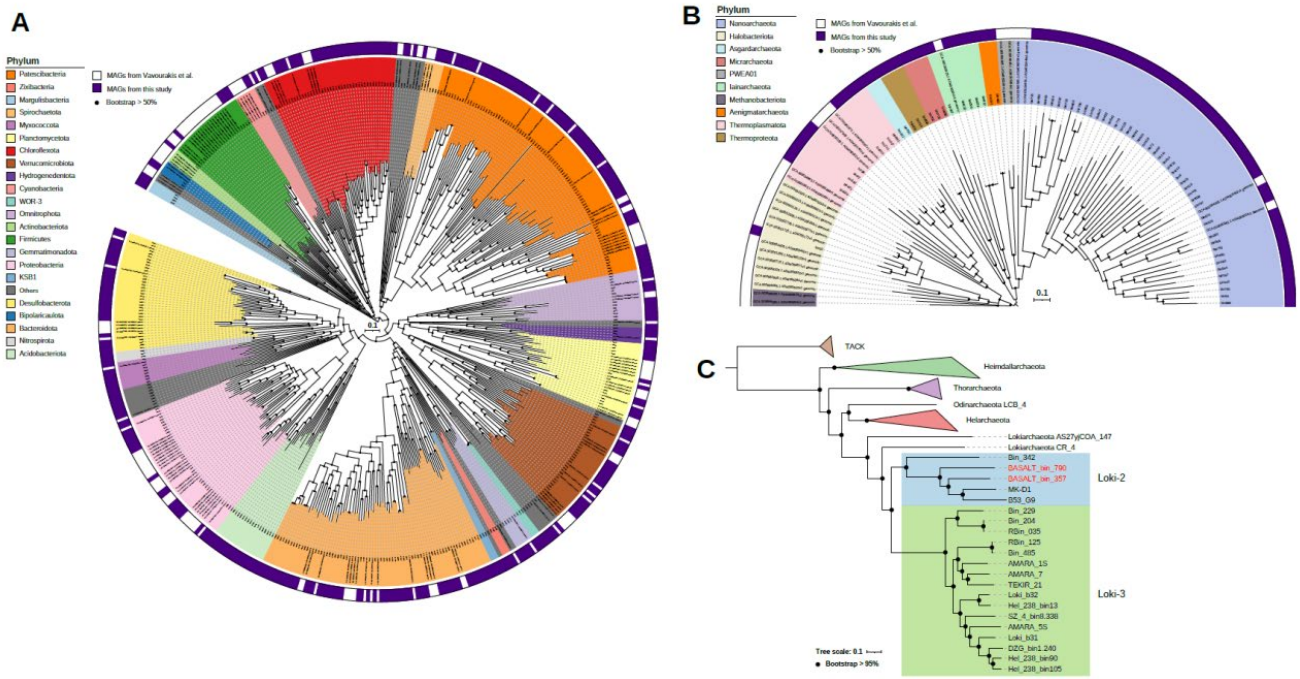

Figure 3. Phylogenetic trees of **A)** bacterial MAGs from Vavourakis et al. (2018) and this study, **B)** archaeal MAGs from Vavourakis et al. (2018) and this study, and **C)** Maximum-likelihood tree of Asgardarchaeotal MAGs based on protein encoded genes from the whole genome. The unrooted phylogenetic trees in A) and B) were constructed with Fasttree, while the Maximum-likelihood tree in C) was constructed with PHYML and re-rooted with superphylum TACK. The two Lokiarchaeota MAGs found in this study were highlighted with red in C), and all genomes used to create trees that not obtained from this study were listed in Table S2.

Newly discovered Lokiarchaeota species from a deep-inland non-marine hypersaline lake.

Using four metagenome samples, BASALT pipeline expanded 421 of known species on prokaryotic

311 phylogenetic tree with samples from one Salt Lake. Remarkably, two MAGs classified as
312 Lokiarchaeota belongs to the superphylum Asgardarchaeota, were also observed in our results.
313 Although previous study has reported Asgardarchaeota phyla found in hypersaline lakes (Bulzu et al.
314 2019), to the best of our knowledge, this is the first time that archaeal phylum Lokiarchaeota was found
315 from the deep inland non-marine samples. Comparing with other MAGs/isolates obtained in previous
316 studies, the two MAGs found in our study were grouped with Loki-2 MAGs/isolates (Figure 3C), next
317 to *Ca. Prometheoarchaeum syntrophicum*, a strain isolated from a deep-sea sediment sample at Nankai
318 Trough, Japan (Imachi et al. 2020). Interestingly, other Loki-2 MAGs were found globally, including
319 Bin_342 from Shark Bay, Australia (Wong et al. 2020) and B53_G9 from Guaymas Basin, US (Seitz
320 et al. 2019), suggesting that Loki-2 species were widely distributed not only in marine sediments but
321 also in the deep-inland terrestrial environment.

322

323 **Discussion**

324 BASALT is superior in quality and number of MAGs on low (132 genomes) to medium (596 genomes)
325 complexity samples. In regards of MAG quality assessment, CheckM (Parks et al. 2015) is widely
326 used in a vast majority of studies. However, in the presence of standard CAMI datasets, we calculated
327 the MAG quality against the corresponding genomes that can result in more accurate evaluations.
328 Notably, our dereplication module implemented in the integration step can efficiently remove
329 redundant bins that generated in co-assembly and bin selection steps, which was evidenced in the test
330 analysis using both CAMI-medium and CAMI-high datasets (Figure 2A). Although there are other
331 redundancy removal methods such as dRep (Olm et al. 2017), result suggested that redundant genomes
332 cannot be efficiently identified and removed using dRep on CAMI-medium or CAMI-high datasets
333 (Table S1), suggesting that BASALT Bin Dereplication gains more advantages in removing redundant
334 bins under higher complexed samples. Due to the scarcity of standard synthesized community with

335 high complexity to date, further works testing the efficiency of Bin Dereplication module on the
336 standardized samples with high complexity are needed.

337 BASALT-integrated Bin Dereplication module can efficiently remove redundant bins generated by
338 binning tools. However, due to the major impediments of short-fragmented technology of next-
339 generation sequencing (NGS) and post sequencing algorithm, recovered MAGs cannot specify
340 differences of genomes at strain level with high similarity. While long read sequencing such as ONT
341 has become more popular in the current metagenomic studies (Jain et al. 2016), high error rates still
342 required to be rectified by NGS. In this study, third-generation sequences were innovatively integrated
343 into our toolkit where long reads can be used to amend sequences and fill gaps on assembled genomes,
344 which can improve the overall quality of bins and increase the number of high-qualitied MAGs.
345 Although standard dataset with high complexity is currently not available in the database, our case
346 study revealed that Salt Lake sediments can be considered as samples with relatively high complexity
347 (6,993 ZOTUs from 16S rRNA gene amplicons), which was comparable with other studies on soil
348 samples regardless the primer selection (Fulthorpe et al. 2008, Xiong et al. 2021). In the context of
349 high complexed samples of Salt Lake sediments, BASALT could also efficiently conduct reads
350 utilization in metagenomic binning with 26.9% mapped sequences, which to some extent helped to
351 resolve the difficulty raised in the EMP project (Nayfach et al. 2020). Prospectively, the trend in the
352 development of third-generation sequencing has inspired that further exploitation of long-read
353 sequences can increase the resolution of MAGs at strain or single nucleotide polymorphism (SNP),
354 which may boost the outcome of recovered genomes in high complexity samples. Therefore, future
355 development should focus on the combination of NGS and TGS to improve the efficiency of binning,
356 which consequently expand our knowledge on the tree of life.

357 In addition to the BASALT toolkits introduced in this study, one major finding in the case study was
358 the discovery of two novel Lokiarchaeota genomes from the sediment samples of Aiding Lake.
359 Lokiarchaeota belongs to a recently discovered superphylum Asgardarchaeota, which is a hot topic

linked to the origin of eukaryotes (Spang et al. 2018). To date, candidate species of Lokiarchaeota were universally found near deep sea hydrothermal vents and marine sediments (Spang et al. 2015, Spang et al. 2018, Hoshino et al. 2020, Wong et al. 2020, Yin et al. 2020). A recent study has found candidate Lokiarchaeota present in hypersaline lakes near Black Sea (Bulzu et al. 2019), whereas our study highlighted the first time that Loki-2 species were found from deep-inland hypersaline lake sediments. Given the genetic analysis on Lokiarchaeota along with other candidate Asgardarchaeota species (Zaremba-Niedzwiedzka et al. 2017, Seitz et al. 2019, Imachi et al. 2020, Wong et al. 2020, Yin et al. 2020) have suggested that candidate Lokiarchaeota species were adaptive in marine environment with distinct metabolic pathway, such as lignin or protein degradations. Thus, it was unlikely that candidate Loki-2 species were newly emerged in the deep-inland hypersaline lake. Therefore, the discovery in this study might have provided a landmark that candidate Lokiarchaeota species might exist in the ancient age before the plate movement event occurred. However, insufficient MAGs/isolates revealed to date hampered us to make rigid conclusions, that more investigation on this group of archaea is critically required in the future studies.

Methods

Overview of BASALT

BASALT is a versatile toolkit that recovers, compares and optimizes MAGs across a series of assemblies assembled from short-read, long-read or hybrid strategies. We established five homebrew algorithms to carry out Core Contigs Identification (CCI), Bin Depth Normalization, Outlier Removal (OR), Contigs Retrieval, and restrained overlap-layout-consensus (rOLC). These algorithms consist three core modules of BASALT, such as Bin Dereplication, Bin Refinement and Bin Reassembly modules. Besides, BASALT contains an autobinning module that uses mapping tools (e.g. bowtie2, Langdon 2015) and binners (e.g. MetaBAT2, Maxbin2, and CONCOCT) to generate a raw hybrid bin-

384 set after input of assemblies (Figure 1).

385

386 **Dereplication of redundant bins**

387 Incompleteness and contamination of MAGs would hinder the dereplication of bins from the hybrid
388 bin-set. We developed an effectively strategy that can remove most of the potential contaminated
389 sequences while large number of sequences are still kept to carrying out precise redundancy
390 identification. Different from previously reported genome-wide ANI-based and marker gene- based
391 de-replicating methods such as dRep (Olm et al. 2017), the present method firstly generated a core
392 contig pool by filtering out potentially contaminated contigs of target bins. The depth and
393 tetranucleotide frequency (TNF) value of the selected contigs ranked from a range of 25 to 75
394 percentile of all the contigs of target bins. Then, selected bins were grouped into different raw bin-sets
395 based on overall similarity of core contigs. Secondly, we evaluated the sequencing depth discrepancy
396 among bins across different bin-sets to ensure the correct identification of redundant bins with relative
397 low similarity. The average depth of one bin should be equivalent to the average depth of the core
398 contigs of this bin. For neutralizing the sequencing depth discrepancy yielded by mapping the same
399 reads to different assemblies, we designed a method to calculate the normalization ratio between two
400 possibly redundant bins, which identifies near-identical sequences (99.8% similarity across longer than
401 50% of the whole length of sequence) between two potential redundant bins as candidate bins. A depth
402 normalization ratio between candidate bins was then calculated by using the depth of these contigs,
403 which was then used to neutralize the average depth of candidate bins. Those candidate bins with
404 similar average sequencing depth (delta ≤ 10%) were considered as redundant bins to be removed.
405 Finally, the bin with better quality value (completeness – 5* contamination) estimated by CheckM
406 (Parks et al. 2015) was kept being the better bin for further refinement and reassembly.

407

Refinement

BASALT refinement module contains two adversary processes: Outlier Removal (OR) and Contig Retrieval. To effectively remove contaminated contigs from a certain bin, we designed an outlier removal algorithm that removes contigs with an outlier value of sequencing depth or TNF based on an interquartile range (Formula 1), while different thresholds (k) were set (e.g. 1, 1.5, 3) to determine these contigs. In the context of bin quality, OR keeps bins with higher quality value, while bins with lower quality were discarded. If no refined bin with higher quality than the original bin was generated, OR would acquiescently eliminate sequences marked as depth or TNF outliers under the threshold of 3. Notably, the default setting of OR mainly removes contaminated sequences, but it may cause an unnecessary removal of contigs due to restricted threshold.

Formula 1:

$$x_i > Q3 + k(IQR) \vee x_i < Q1 - k(IQR)$$

In this formula, Q1 and Q3 stands for 25 and 75 percentiles of all contigs, where IQR (interquartile ranges) was calculated by Q3 – Q1. $k \geq 0$.

Contig Retrieval algorithm was designed to retrieve sequences that have not been clustered into the target bin in the binning process, especially multicopy sequences or unnecessarily removed sequences by Outlier Removal. Contig Retrieval identifies contigs that potentially connected to existing sequences in the target bin. These candidate contigs were further assessed by an interquartile range method to remove depth or TNF outliers as described above and connected to the target bin by paired-end tracking (Albertsen et al. 2013) or long-read mapped method, forming a refined bin. Refined bins were expected to have higher quality value than target bins which were further selected to form a refined bin-set for further reassembly.

432 **Reassembly**

433 BASALT reassembly module includes a restrained overlap-layout-consensus (rOLC) process and a
434 reassembly process. The rOLC algorithm was designed to retrieve sequence which was not included
435 in the BASALT binning and refinement processes. Specifically, this process re-utilized sequences from
436 redundant bins identified and removed from the dereplication module to overlap the sequences from
437 the target bin. Using a loose threshold (overlap length: 300 bp; similarity: 99%), rOLC algorithm
438 aggressively recorded the redundant candidate sequences removed from the target bin in the previous
439 steps. As rOLC process may increase the contamination of sequences, a reassembly step was
440 implemented after rOLC to amend the contamination caused by rOLC, and more importantly, to
441 precisely elongate the length of sequences in the target bin. In the reassembly process, short-read or
442 long-read sequences were extracted from datasets by Bowtie2 and Minimap2, respectively (Langdon
443 2015, Li 2018). Three state-of-art assemblers were implemented in the reassembly step: SPAdes, FLYe,
444 and Unicycler (Bankevich et al. 2012, Wick et al. 2017, Kolmogorov et al. 2019) to carry out short-
445 read reassembly, long-read reassembly and hybrid reassembly, respectively. A final bin selecting
446 process was exploited to select the best bins from the reassembly step to form the final bins for post-
447 binning analysis.

448

449 **Sample collection**

450 Salt Lake sediment samples were collected in July 2018 from Aiding Lake, an arid region in Turpan
451 City, Xinjiang Uygur Autonomous Region (42°52′9″ N, 89°03′5″ E). Briefly, about 50 grams of
452 sediment samples (n = 4) were randomly collected at 0-10 cm depth in the lake into sterile 50 ml falcon
453 tubes. Samples were immediately placed on dry ice before brought to laboratory and transferred to -
454 80 °C freezer until further DNA extraction was performed.

455

456 **DNA extraction and sequencing**

457 Frozen stored sediment samples (~250 mg dry weight per sample) was used to extract genomic DNA
458 using DNeasy PowerSoil Kit (Qiagen, Hilden, Germany), following the manufacturer's instructions.
459 Extracted DNA was quality checked by NanoDrop 2000 (Thermo Fisher Scientific, Waltham,
460 Massachusetts, US), quantity checked by Qubit Fluorometer (Thermo Fisher Scientific) and PCR
461 checked to confirm the amplifiability.

462 For 16S rRNA gene amplicon sequencing, barcode as a marker for each sample DNA was added at the
463 5' end of primers targeting V4 region for bacterial and archaeal communities (515F-806R, Caporaso
464 et al. 2012). Sequencing was performed at MAGIGENE, Guangzhou, China on an Illumina NovaSeq
465 6000 platform (2 × 250 bp paired end chemistry).

466 For shotgun metagenomics sequencing, quantity and quality checked genomic DNA was sent to
467 Novegene Co., Ltd, Nanjing, China on an Illumina NovaSeq (2 × 150 bp paired end chemistry).

468

469 **Sequencing processing**

470 To evaluate the efficiency of BASALT, standard Critical Assessment of Metagenome Interpretation
471 (CAMI) datasets including a simple-complexity (132 genomes, CAMI-medium) and a medium-
472 complexity (596 genomes, CAMI-high) synthesized communities were downloaded from
473 (https://data.cami-challenge.org/participate) (Sczyrba et al. 2017). Raw paired-end reads were initially
474 filtered using fastp (Chen et al. 2018). Fifty percent of bases were filtered based on a minimum quality
475 score of 5 and sequence length of 150 bp, allowing no ambiguous bases. Clean reads were individually
476 and co-assembled using SPAdes (version3.14.1, Bankevich et al. 2012) into contigs specifying k-mer
477 sizes of 21, 33, 55, 77 and finally reserved contigs > 1,000 bps. To compare with other binners/toolkits,
478 filtered contigs were processed with DASTool, VAMB, metaWRAP and BASALT, respectively. The
479 redundancy, completeness and contamination of the MAGs were calculated against standard CAMI

480 datasets using a homebrew script *Bin_quality_evaluation.py* available on github
481 (https://github.com/EMBL-PKU/BASALT) to ensure high accuracy of results obtained from the four
482 binners/toolkits. High-quality MAGs (completeness - 5*contamination ≥ 50%) were kept for further
483 statistical analysis, whereas bins did not meet the quality were discarded.

484 For Aiding Lake sediment samples, raw 16S rRNA gene amplicon sequences were processed using
485 Quantitative Insights Into Microbial Ecology (QIIME2) pipeline (http://qiime.org) (Caporaso et al.
486 2010). DADA2 was used to filter low-quality sequences with lengths < 230 bp, remove chimeric
487 sequences, singletons, and join the quality-filtered paired-end reads. Unique sequences (100%
488 similarity) were taxonomically assigned using Naive Bayes classifier against the SILVA 16S rRNA
489 gene reference alignment database (release 123) (Pruesse et al. 2007). To compare the complexity of
490 Salt Lake sediment samples with other high-complexed samples such as soil, sequences were rarefied
491 to an even sampling depth at 10,000 reads per sample, before singleton was removed from the
492 generated OTU table. Overall, a total number of 6,993 ZOTUs (Zero-radius OTUs) were obtained.

493 For shotgun metagenomic sequences of Aiding Lake sediment samples, sequences were processed
494 following the same procedure on CAMI-medium and CAMI-high datasets using BASALT. The
495 completeness and contamination of the MAGs were then estimated using CheckM version 1.1.3 (Parks
496 et al. 2015) with lineage-specific marker genes and default parameters, with only high-quality MAGs
497 (completeness - 5*contamination ≥ 50%) were kept for further analyses.

498

499 **Phylogenetic analysis**

500 The GTDB-Tk version (version1.4.1, Chaumeil et al. 2020) program was used to assign taxonomic
501 classifications to the MAGs (release r95). To make comparison with another study of soda lake samples
502 (Vavourakis et al. 2018), dereplicated MAGs were downloaded from NCBI Assembly database and
503 phylogenetic analyses were conducted based on MAGs from both studies using Fasttree (Price et al.

2010). For phylogenetic analysis of Asgardarchaeota, MAGs/isolates were downloaded from other studies listed in Table S2, and Maximum-likelihood tree was constructed using PHYML version 3.0 (Guindon et al. 2010) with 1000 bootstrap iterations. Phylogenetic trees were visualized and edited in the iTOL (https://itol.embl.de) online platform (Letunic and Bork 2019).

Code availability

All BASALT codes including homebrew scripts for quality checking against standard datasets are available at (https://github.com/EMBL-PKU/BASALT).

Reference

Albertsen, M., P. Hugenholtz, A. Skarshewski, K. L. Nielsen, G. W. Tyson, and P. H. Nielsen. 2013. Genome sequences of rare, uncultured bacteria obtained by differential coverage binning of multiple metagenomes. Nature biotechnology **31**:533-538.

Ali, M., D. R. Shaw, M. Albertsen, and P. E. Saikaly. 2020. Comparative genome-centric analysis of freshwater and marine ANAMMOX cultures suggests functional redundancy in nitrogen removal processes. Frontiers in microbiology **11**:1637.

Almeida, A., S. Nayfach, M. Boland, F. Strozzi, M. Beracochea, Z. J. Shi, K. S. Pollard, E. Sakharova, D. H. Parks, and P. Hugenholtz. 2021. A unified catalog of 204,938 reference genomes from the human gut microbiome. Nature biotechnology **39**:105-114.

Alneberg, J., B. S. Bjarnason, I. de Bruijn, M. Schirmer, J. Quick, U. Z. Ijaz, N. J. Loman, A. F. Andersson, and C. Quince. 2013. CONCOCT: clustering contigs on coverage and composition. arXiv preprint arXiv:1312.4038.

Amid, C., B. T. Alako, V. Balavenkataraman Kadhirvelu, T. Burdett, J. Burgin, J. Fan, P. W. Harrison, S. Holt, A. Hussein, and E. Ivanov. 2020. The European nucleotide archive in 2019. Nucleic acids research **48**:D70-D76.

Anderson, R. E., J. Reveillaud, E. Reddington, T. O. Delmont, A. M. Eren, J. M. McDermott, J. S. Seewald, and J. A. Huber. 2017. Genomic variation in microbial populations inhabiting the marine subseafloor at deep-sea hydrothermal vents. Nature communications **8**:1-11.

Bankevich, A., S. Nurk, D. Antipov, A. A. Gurevich, M. Dvorkin, A. S. Kulikov, V. M. Lesin, S. I. Nikolenko, S. Pham, and A. D. Prjibelski. 2012. SPAdes: a new genome assembly algorithm and its applications to single-cell sequencing. Journal of computational biology **19**:455-477.

Berdjeb, L., T. Pollet, I. Domaizon, and S. Jacquet. 2011. Effect of grazers and viruses on bacterial community structure and production in two contrasting trophic lakes. BMC microbiology **11**:1-18.

Bertrand, D., J. Shaw, M. Kalathiyappan, A. H. Q. Ng, M. S. Kumar, C. Li, M. Dvornicic, J. P. Soldo, J. Y. Koh, and C. Tong. 2019. Hybrid metagenomic assembly enables high-resolution analysis of resistance determinants and mobile elements in human microbiomes. Nature biotechnology **37**:937-944.

Bulzu, P.-A., A.-Ş. Andrei, M. M. Salcher, M. Mehrshad, K. Inoue, H. Kandori, O. Beja, R. Ghai, and H. L. Banciu. 2019.

Casting light on Asgardarchaeota metabolism in a sunlit microoxic niche. Nature microbiology **4**:1129-1137.

Caporaso, J. G., J. Kuczynski, J. Stombaugh, K. Bittinger, F. D. Bushman, E. K. Costello, N. Fierer, A. G. Peña, J. K. Goodrich, and J. I. Gordon. 2010. QIIME allows analysis of high-throughput community sequencing data. Nature methods **7**:335-336.

Caporaso, J. G., C. L. Lauber, W. A. Walters, D. Berg-Lyons, J. Huntley, N. Fierer, S. M. Owens, J. Betley, L. Fraser, and M. Bauer. 2012. Ultra-high-throughput microbial community analysis on the Illumina HiSeq and MiSeq platforms. The ISME journal **6**:1621-1624.

Chaumeil, P.-A., A. J. Mussig, P. Hugenholtz, and D. H. Parks. 2020. GTDB-Tk: a toolkit to classify genomes with the Genome Taxonomy Database. Oxford University Press.

Chen, S., Y. Zhou, Y. Chen, and J. Gu. 2018. fastp: an ultra-fast all-in-one FASTQ preprocessor. Bioinformatics **34**:i884-i890.

Easson, C. G., and J. V. Lopez. 2019. Depth-Dependent environmental drivers of microbial plankton community structure in the Northern Gulf of Mexico. Frontiers in microbiology **9**:3175.

Eze, M. O., S. A. Lütgert, H. Neubauer, A. Balouri, A. A. Kraft, A. Sieven, R. Daniel, and B. Wemheuer. 2020. Metagenome assembly and metagenome-assembled genome sequences from a historical oil field located in Wietze, Germany. Microbiology Resource Announcements **9**.

Finstad, K. M., A. J. Probst, B. C. Thomas, G. L. Andersen, C. Demergasso, A. Echeverría, R. G. Amundson, and J. F. Banfield. 2017. Microbial community structure and the persistence of cyanobacterial populations in salt crusts of the hyperarid Atacama Desert from genome-resolved metagenomics. Frontiers in microbiology **8**:1435.

Fulthorpe, R. R., L. F. Roesch, A. Riva, and E. W. Triplett. 2008. Distantly sampled soils carry few species in common. The ISME journal **2**:901-910.

Glasl, B., D. G. Bourne, P. R. Frade, T. Thomas, B. Schaffelke, and N. S. Webster. 2019. Microbial indicators of environmental perturbations in coral reef ecosystems. Microbiome **7**:1-13.

Guan, T.-W., Y.-J. Lin, M.-Y. Ou, and K.-B. Chen. 2020. Isolation and diversity of sediment bacteria in the hypersaline aiding lake, China. PLoS One **15**:e0236006.

Guindon, S., J.-F. Dufayard, V. Lefort, M. Anisimova, W. Hordijk, and O. Gascuel. 2010. New algorithms and methods to estimate maximum-likelihood phylogenies: assessing the performance of PhyML 3.0. Systematic biology **59**:307-321.

Hoshino, T., H. Doi, G.-I. Uramoto, L. Wörmer, R. R. Adhikari, N. Xiao, Y. Morono, S. D'Hondt, K.-U. Hinrichs, and F. Inagaki. 2020. Global diversity of microbial communities in marine sediment. Proceedings of the national academy of sciences **117**:27587-27597.

Howe, A. C., J. K. Jansson, S. A. Malfatti, S. G. Tringe, J. M. Tiedje, and C. T. Brown. 2014. Tackling soil diversity with the assembly of large, complex metagenomes. Proceedings of the national academy of sciences **111**:4904-4909.

Hug, L. A., B. J. Baker, K. Anantharaman, C. T. Brown, A. J. Probst, C. J. Castelle, C. N. Butterfield, A. W. Hernsdorf, Y. Amano, and K. Ise. 2016. A new view of the tree of life. Nature microbiology **1**:1-6.

Imachi, H., M. K. Nobu, N. Nakahara, Y. Morono, M. Ogawara, Y. Takaki, Y. Takano, K. Uematsu, T. Ikuta, and M. Ito. 2020. Isolation of an archaeon at the prokaryote–eukaryote interface. Nature **577**:519-525.

Jain, M., H. E. Olsen, B. Paten, and M. Akeson. 2016. The Oxford Nanopore MinION: delivery of nanopore sequencing to the genomics community. Genome biology **17**:1-11.

Kang, D. D., F. Li, E. Kirton, A. Thomas, R. Egan, H. An, and Z. Wang. 2019. MetaBAT 2: an adaptive binning algorithm for robust and efficient genome reconstruction from metagenome assemblies. PeerJ **7**:e7359.

Kolmogorov, M., J. Yuan, Y. Lin, and P. A. Pevzner. 2019. Assembly of long, error-prone reads using repeat graphs. Nature biotechnology **37**:540-546.

Kroeger, M. E., T. O. Delmont, A. M. Eren, K. M. Meyer, J. Guo, K. Khan, J. L. Rodrigues, B. J. Bohannan, S. G. Tringe,

583 and C. D. Borges. 2018. New biological insights into how deforestation in Amazonia affects soil microbial
584 communities using metagenomics and metagenome-assembled genomes. Frontiers in microbiology **9**:1635.
585 Langdon, W. B. 2015. Performance of genetic programming optimised Bowtie2 on genome comparison and analytic testing
586 (GCAT) benchmarks. BioData mining **8**:1-7.
587 Laver, T., J. Harrison, P. O'neill, K. Moore, A. Farbos, K. Paszkiewicz, and D. J. Studholme. 2015. Assessing the
588 performance of the oxford nanopore technologies minion. Biomolecular detection and quantification **3**:1-8.
589 Letunic, I., and P. Bork. 2019. Interactive Tree Of Life (iTOL) v4: recent updates and new developments. Nucleic acids
590 research **47**:W256-W259.
591 Lewis, W. H., G. Tahon, P. Geesink, D. Z. Sousa, and T. J. Ettema. 2020. Innovations to culturing the uncultured microbial
592 majority. Nature Reviews Microbiology:1-16.
593 Li, D., C.-M. Liu, R. Luo, K. Sadakane, and T.-W. Lam. 2015. MEGAHIT: an ultra-fast single-node solution for large and
594 complex metagenomics assembly via succinct de Bruijn graph. Bioinformatics **31**:1674-1676.
595 Li, H. 2018. Minimap2: pairwise alignment for nucleotide sequences. Bioinformatics **34**:3094-3100.
596 Liang, Z., J. Shi, C. Wang, J. Li, D. Liang, E. L. Yong, Z. He, and S. Wang. 2020. Genome-centric metagenomic insights
597 into the impact of alkaline/acid and thermal sludge pretreatment on the microbiome in digestion sludge. Applied
598 and environmental microbiology **86**.
599 Nascimento Lemos, L., L. Manoharan, L. William Mendes, A. Monteiro Venturini, V. Satler Pylro, and S. M. Tsai. 2020.
600 Metagenome assembled-genomes reveal similar functional profiles of CPR/Patescibacteria phyla in soils.
601 Environmental microbiology reports **12**:651-655.
602 Nayfach, S., B. Rodriguez-Mueller, N. Garud, and K. S. Pollard. 2016. An integrated metagenomics pipeline for strain
603 profiling reveals novel patterns of bacterial transmission and biogeography. Genome research **26**:1612-1625.
604 Nayfach, S., S. Roux, R. Seshadri, D. Udwary, N. Varghese, F. Schulz, D. Wu, D. Paez-Espino, I.-M. Chen, and M.
605 Huntemann. 2020. A genomic catalog of Earth's microbiomes. Nature biotechnology:1-11.
606 Nishiyama, E., K. Higashi, H. Mori, K. Suda, H. Nakamura, S. Omori, S. Maruyama, Y. Hongoh, and K. Kurokawa. 2018.
607 The relationship between microbial community structures and environmental parameters revealed by
608 metagenomic analysis of hot spring water in the Kirishima Area, Japan. Frontiers in bioengineering and
609 biotechnology **6**:202.
610 Nissen, J. N., J. Johansen, R. L. Allesøe, C. K. Sønderby, J. J. A. Armenteros, C. H. Grønbech, L. J. Jensen, H. B. Nielsen,
611 T. N. Petersen, and O. Winther. 2021. Improved metagenome binning and assembly using deep variational
612 autoencoders. Nature biotechnology:1-6.
613 Olm, M. R., C. T. Brown, B. Brooks, and J. F. Banfield. 2017. dRep: a tool for fast and accurate genomic comparisons that
614 enables improved genome recovery from metagenomes through de-replication. The ISME journal **11**:2864-2868.
615 Parks, D. H., M. Chuvochina, D. W. Waite, C. Rinke, A. Skarshewski, P.-A. Chaumeil, and P. Hugenholtz. 2018. A
616 standardized bacterial taxonomy based on genome phylogeny substantially revises the tree of life. Nature
617 biotechnology **36**:996-1004.
618 Parks, D. H., M. Imelfort, C. T. Skennerton, P. Hugenholtz, and G. W. Tyson. 2015. CheckM: assessing the quality of
619 microbial genomes recovered from isolates, single cells, and metagenomes. Genome research **25**:1043-1055.
620 Parks, D. H., C. Rinke, M. Chuvochina, P.-A. Chaumeil, B. J. Woodcroft, P. N. Evans, P. Hugenholtz, and G. W. Tyson.
621 2017. Recovery of nearly 8,000 metagenome-assembled genomes substantially expands the tree of life. Nature
622 microbiology **2**:1533-1542.
623 Pasolli, E., F. Asnicar, S. Manara, M. Zolfo, N. Karcher, F. Armanini, F. Beghini, P. Manghi, A. Tett, and P. Ghensi. 2019.
624 Extensive unexplored human microbiome diversity revealed by over 150,000 genomes from metagenomes
625 spanning age, geography, and lifestyle. Cell **176**:649-662. e620.
626 Peng, Y., H. C. Leung, S.-M. Yiu, and F. Y. Chin. 2012. IDBA-UD: a de novo assembler for single-cell and metagenomic

sequencing data with highly uneven depth. Bioinformatics **28**:1420-1428.

Price, M. N., P. S. Dehal, and A. P. Arkin. 2010. FastTree 2–approximately maximum-likelihood trees for large alignments. PLoS One **5**:e9490.

Pruesse, E., C. Quast, K. Knittel, B. M. Fuchs, W. Ludwig, J. Peplies, and F. O. Glöckner. 2007. SILVA: a comprehensive online resource for quality checked and aligned ribosomal RNA sequence data compatible with ARB. Nucleic Acids Res **35**.

Ransom-Jones, E., A. J. McCarthy, S. Haldenby, J. Doonan, and J. E. McDonald. 2017. Lignocellulose-degrading microbial communities in landfill sites represent a repository of unexplored biomass-degrading diversity. Msphere **2**.

Reji, L., B. B. Tolar, J. M. Smith, F. Chavez, and C. Francis. 2020. Genome-resolved metagenomics reveals lineage-specific metabolic strategies within marine nitrifier subpopulations.*in* Ocean Sciences Meeting 2020. AGU.

Rinke, C., P. Schwientek, A. Sczyrba, N. N. Ivanova, I. J. Anderson, J.-F. Cheng, A. Darling, S. Malfatti, B. K. Swan, and E. A. Gies. 2013. Insights into the phylogeny and coding potential of microbial dark matter. Nature **499**:431-437.

Sczyrba, A., P. Hofmann, P. Belmann, D. Koslicki, S. Janssen, J. Dröge, I. Gregor, S. Majda, J. Fiedler, and E. Dahms. 2017. Critical assessment of metagenome interpretation—a benchmark of metagenomics software. Nature methods **14**:1063-1071.

Seitz, K. W., N. Dombrowski, L. Eme, A. Spang, J. Lombard, J. R. Sieber, A. P. Teske, T. J. Ettema, and B. J. Baker. 2019. Asgard archaea capable of anaerobic hydrocarbon cycling. Nature communications **10**:1-11.

Song, W.-Z., and T. Thomas. 2017. Binning_refiner: improving genome bins through the combination of different binning programs. Bioinformatics **33**:1873-1875.

Spang, A., L. Eme, J. H. Saw, E. F. Caceres, K. Zaremba-Niedzwiedzka, J. Lombard, L. Guy, and T. J. Ettema. 2018. Asgard archaea are the closest prokaryotic relatives of eukaryotes. PLoS genetics **14**:e1007080.

Spang, A., J. H. Saw, S. L. Jørgensen, K. Zaremba-Niedzwiedzka, J. Martijn, A. E. Lind, R. Van Eijk, C. Schleper, L. Guy, and T. J. Ettema. 2015. Complex archaea that bridge the gap between prokaryotes and eukaryotes. Nature **521**:173-179.

Stewart, R. D., M. D. Auffret, A. Warr, A. H. Wiser, M. O. Press, K. W. Langford, I. Liachko, T. J. Snelling, R. J. Dewhurst, and A. W. Walker. 2018. Assembly of 913 microbial genomes from metagenomic sequencing of the cow rumen. Nature communications **9**:1-11.

Temperton, B., and S. J. Giovannoni. 2012. Metagenomics: microbial diversity through a scratched lens. Current opinion in microbiology **15**:605-612.

Thompson, L. R., J. G. Sanders, D. McDonald, A. Amir, J. Ladau, K. J. Locey, R. J. Prill, A. Tripathi, S. M. Gibbons, and G. Ackermann. 2017. A communal catalogue reveals Earth's multiscale microbial diversity. Nature **551**:457-463.

Tully, B. J., E. D. Graham, and J. F. Heidelberg. 2018. The reconstruction of 2,631 draft metagenome-assembled genomes from the global oceans. Scientific data **5**:1-8.

Tyson, G. W., J. Chapman, P. Hugenholtz, E. E. Allen, R. J. Ram, P. M. Richardson, V. V. Solovyev, E. M. Rubin, D. S. Rokhsar, and J. F. Banfield. 2004. Community structure and metabolism through reconstruction of microbial genomes from the environment. Nature **428**.

Uritskiy, G. V., J. DiRuggiero, and J. Taylor. 2018. MetaWRAP—a flexible pipeline for genome-resolved metagenomic data analysis. Microbiome **6**:1-13.

Vavourakis, C. D., A.-S. Andrei, M. Mehrshad, R. Ghai, D. Y. Sorokin, and G. Muyzer. 2018. A metagenomics roadmap to the uncultured genome diversity in hypersaline soda lake sediments. Microbiome **6**:1-18.

Wang, M., C. R. Beck, A. C. English, Q. Meng, C. Buhay, Y. Han, H. V. Doddapaneni, F. Yu, E. Boerwinkle, and J. R. Lupski. 2015. PacBio-LITS: a large-insert targeted sequencing method for characterization of human disease-associated chromosomal structural variations. BMC genomics **16**:1-12.

Wang, Z., Z. Wang, Y. Y. Lu, F. Sun, and S. Zhu. 2019. SolidBin: improving metagenome binning with semi-supervised

671 normalized cut. Bioinformatics **35**:4229-4238.
672 Wick, R. R., L. M. Judd, C. L. Gorrie, and K. E. Holt. 2017. Unicycler: resolving bacterial genome assemblies from short
673 and long sequencing reads. PLoS computational biology **13**:e1005595.
674 Wong, H. L., F. I. MacLeod, R. A. White, P. T. Visscher, and B. P. Burns. 2020. Microbial dark matter filling the niche in
675 hypersaline microbial mats. Microbiome **8**:1-14.
676 Wu, Y.-W., B. A. Simmons, and S. W. Singer. 2016. MaxBin 2.0: an automated binning algorithm to recover genomes from
677 multiple metagenomic datasets. Bioinformatics **32**:605-607.
678 Xiong, C., Y. G. Zhu, J. T. Wang, B. Singh, L. L. Han, J. P. Shen, P. P. Li, G. B. Wang, C. F. Wu, and A. H. Ge. 2021. Host
679 selection shapes crop microbiome assembly and network complexity. New Phytologist **229**:1091-1104.
680 Yin, X., M. Cai, Y. Liu, G. Zhou, T. Richter-Heitmann, D. A. Aromokeye, A. C. Kulkarni, R. Nimzyk, H. Cullhed, and Z.
681 Zhou. 2020. Subgroup level differences of physiological activities in marine Lokiarchaeota. The ISME journal:1-
682 14.
683 Yu, G., Y. Jiang, J. Wang, H. Zhang, and H. Luo. 2018. BMC3C: binning metagenomic contigs using codon usage, sequence
684 composition and read coverage. Bioinformatics **34**:4172-4179.
685 Zaremba-Niedzwiedzka, K., E. F. Caceres, J. H. Saw, D. Bäckström, L. Juzokaite, E. Vancaester, K. W. Seitz, K.
686 Anantharaman, P. Starnawski, and K. U. Kjeldsen. 2017. Asgard archaea illuminate the origin of eukaryotic
687 cellular complexity. Nature **541**:353-358.

688

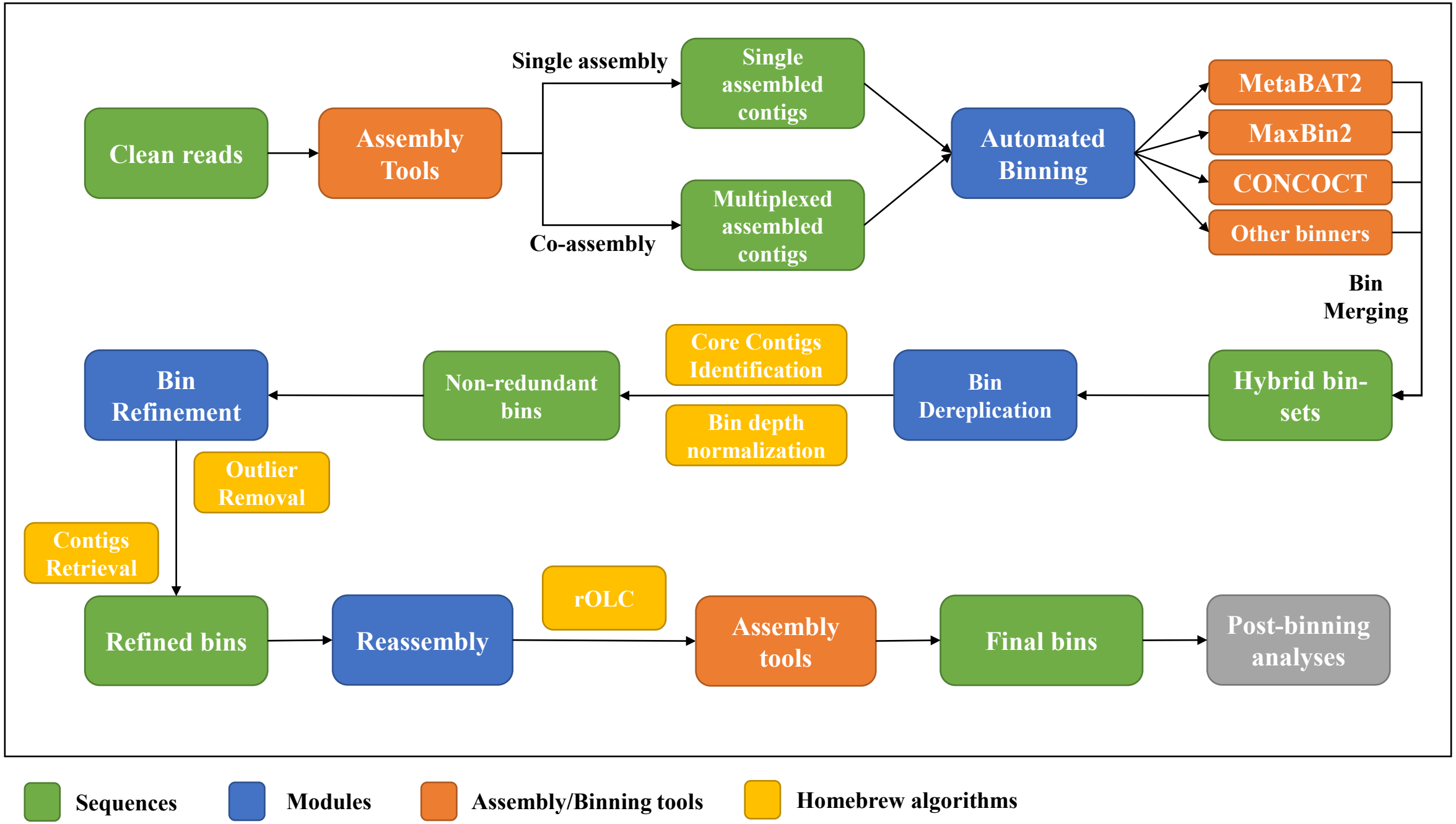
Clean reads
Assembly Tools
Single assembly
Co-assembly
Single assembled contigs
Multiplexed assembled contigs
Automated Binning
MetaBAT2
MaxBin2
CONCOCT
Other binners
Bin Merging
Hybrid bin-sets
Bin Dereplication
Core Contigs Identification
Bin depth normalization
Non-redundant bins
Bin Refinement
Outlier Removal
Contigs Retrieval
Refined bins
Reassembly
rOLC
Assembly tools
Final bins
Post-binning analyses
Sequences
Modules
Assembly/Binning tools
Homebrew algorithms

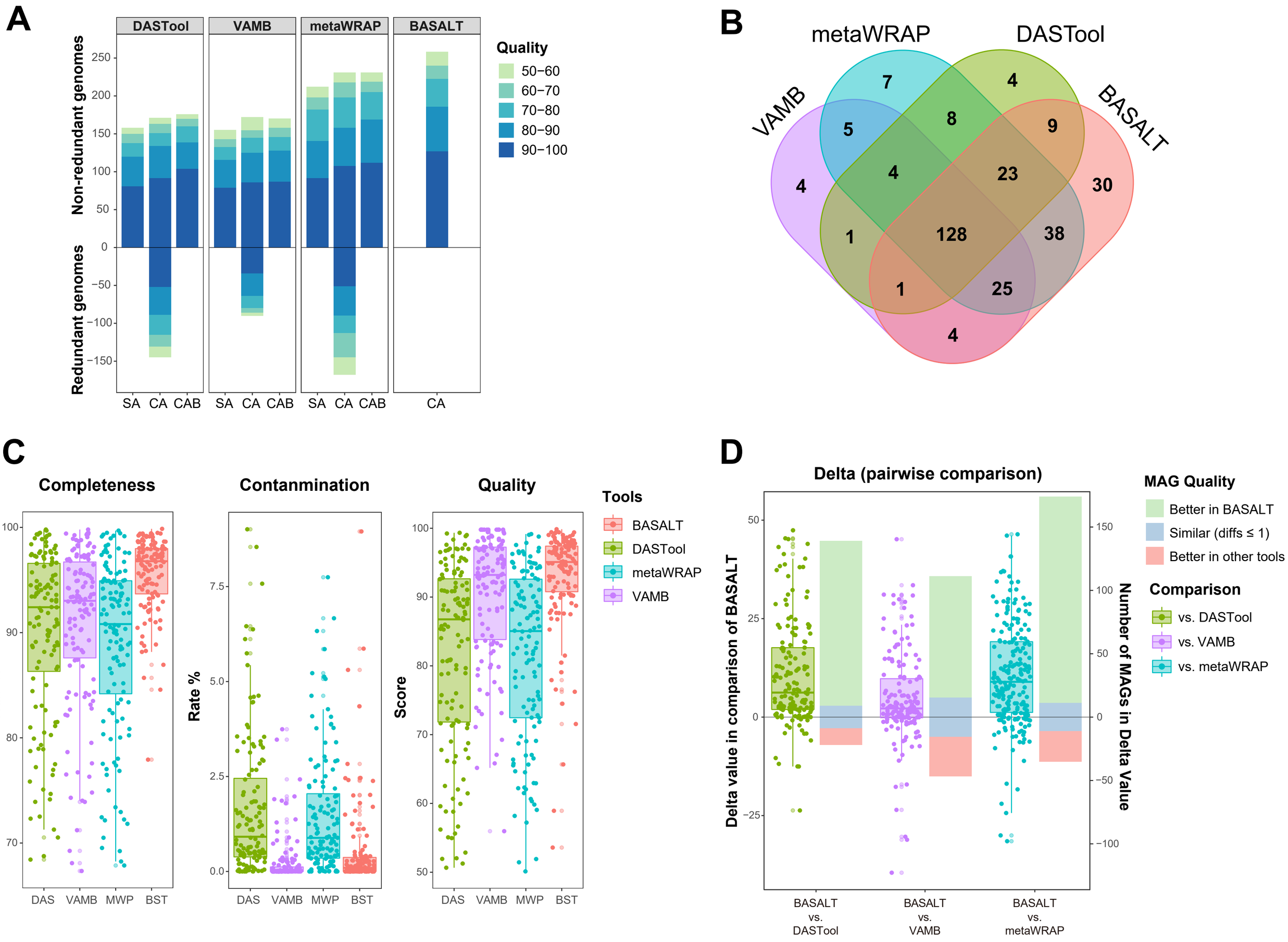
A
DASTool
VAMB
metaWRAP
BASALT
Non-redundant genomes
Redundant genomes
250
200
150
100
50
0
−50
−100
−150
SA CA CAB
SA CA CAB
SA CA CAB
CA
Quality
50−60
60−70
70−80
80−90
90−100
B
metaWRAP
DASTool
VAMB
BASALT
7
4
5
8
9
4
4
23
30
1
128
38
1
25
4
C
Completeness
Contanmination
Quality
Rate %
Rate %
Score
DAS VAMB MWP BST
Tools
BASALT
DASTool
metaWRAP
VAMB
D
Delta (pairwise comparison)
Delta value in comparison of BASALT
Number of MAGs in Delta Value
BASALT vs. DASTool
BASALT vs. VAMB
BASALT vs. metaWRAP
MAG Quality
Better in BASALT
Similar (diffs ≤ 1)
Better in other tools
Comparison
vs. DASTool
vs. VAMB
vs. metaWRAP

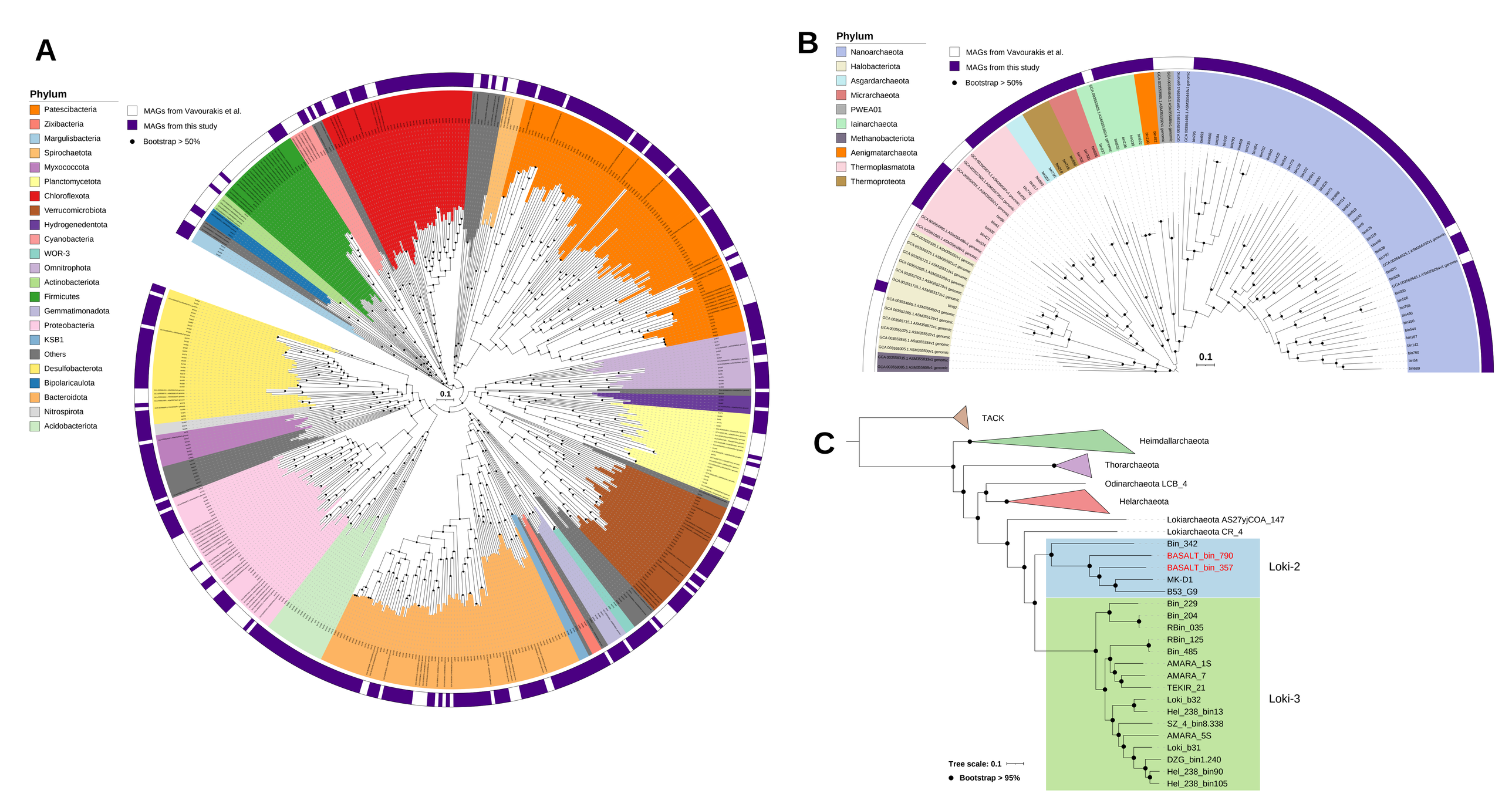
A
Phylum
Patescibacteria
Zixibacteria
Margulisbacteria
Spirochaetota
Myxococcota
Planctomycetota
Chloroflexota
Verrucomicrobiota
Hydrogenedentota
Cyanobacteria
WOR-3
Omnitrophota
Actinobacteriota
Firmicutes
Gemmatimonadota
Proteobacteria
KSB1
Others
Desulfobacterota
Bipolaricaulota
Bacteroidota
Nitrospirota
Acidobacteriota
MAGs from Vavourakis et al.
MAGs from this study
Bootstrap > 50%
0.1
B
Phylum
Nanoarchaeota
Halobacteriota
Asgardarchaeota
Micrarchaeota
PWEA01
Iainarchaeota
Methanobacteriota
Aenigmatarchaeota
Thermoplasmatota
Thermoproteota
MAGs from Vavourakis et al.
MAGs from this study
Bootstrap > 50%
0.1
C
TACK
Heimdallarchaeota
Thorarchaeota
Odinarchaeota LCB_4
Helarchaeota
Lokiarchaeota AS27yjCOA_147
Lokiarchaeota CR_4
Bin_342
BASALT_bin_790
BASALT_bin_357
MK-D1
B53_G9
Loki-2
Bin_229
Bin_204
RBin_035
RBin_125
Bin_485
AMARA_1S
AMARA_7
TEKIR_21
Loki_b32
Hel_238_bin13
SZ_4_bin8.338
AMARA_5S
Loki_b31
DZG_bin1.240
Hel_238_bin90
Hel_238_bin105
Loki-3
Tree scale: 0.1
Bootstrap > 95%